Available online at www.sciencedirect.com
SCIENCE DIRECT®
Journal of Chromatography A, 1037 (2004) 411–429
JOURNAL OF CHROMATOGRAPHY A
www.elsevier.com/locate/chroma

Review

Impulse response techniques to measure binary diffusion coefficients under supercritical conditions

Toshitaka Funazukuri [a,*], Chang Yi Kong [b], Seiichiro Kagei [b]

[a] *Department of Applied Chemistry, Institute of Science and Engineering, Chuo University, 1-13-27 Kasuga, Bunkyo-ku, Tokyo 112-8551, Japan*
[b] *Faculty of Environment and Information Sciences, Yokohama National University, 79-7 Tokiwadai, Hodogaya-ku, Yokohama 240-8501, Japan*

Abstract

This review describes impulse response techniques with a curve-fitting method to measure thermodynamic properties, such as binary diffusion coefficient, retention factor, and partial molar volume, under supercritical conditions. Theoretical background, parameter sensitivity, sources of experimental error, noise elimination technique, and the correction of apparent binary diffusion coefficients due to column coiling are discussed based on recent studies, together with data sources and predictive correlations for binary diffusion coefficients.

Keywords: Reviews; Impulse response; Diffusion coefficients; Retention factors; Molar volume; Curve fitting; Supercritical fluid chromatography; Thermodynamic parameters

Contents

* Corresponding author. Tel.: +81-3-3817-1914; fax: +81-3-3817-1895.
E-mail address: funazo@chem.chuo-u.ac.jp (T. Funazukuri).

0021-9673/$ – see front matter © 2004 Elsevier B.V. All rights reserved.
doi:10.1016/j.chroma.2004.03.043

1. Introduction

Measurements of binary diffusion coefficients for various organic compounds in supercritical fluids have been reported for four decades. In the 1960s and 1970s, Tsekhanskaya and coworkers [1,2] determined binary diffusion coefficients of naphthalene in supercritical (SC) carbon dioxide by measuring dissolution rates. The Taylor dispersion method, also called the chromatographic peak broadening method, was first applied by Swaid and Schneider [3] to measure binary diffusion coefficients of benzene and alkylbenzenes in supercritical carbon dioxide. Since then, many measurements under supercritical conditions using this method have been reported [4–6].

In the Taylor dispersion method, theoretical treatment was made by Taylor [7], and further developed by Aris [8]. This technique has been used for binary diffusion coefficients in gaseous, liquid, and supercritical fluids [4–6,9–12]. The technique is a type of transient response method: a delta or delta-like pulse of solute species is injected into a flowing solvent, and the response is measured at a point downstream. Binary diffusion coefficients are obtained from the difference in the variances between the two points.

In general, transient response methods offer advantages over methods conducted under steady-state conditions because measurements of transport properties can be made from small gradients of driving forces, such as from a small change in concentration, and the times required are relatively short when compared with those under steady-state conditions. Thus, the Taylor dispersion method is quite accurate [12] and less time-consuming [4,12] than steady-state methods.

For the Taylor dispersion method, a small quantity of solute is injected into a fluid. A gaseous or non-viscous liquid solute is injected through an ordinary six-way valve or HPLC injector. However, the injection of a viscous liquid or a solid solute can be difficult. Usually, these solutes are injected as a solution dissolved in a supercritical fluid or an organic solvent. In the former, difficulty is often encountered in adjusting the quantity injected because solubility changes drastically over the pressure range. In the latter, the effect of the organic solvent is ambiguous, although the response curves are not influenced optically by the organic solvent which substantially has no UV or UV–Vis absorption. To overcome problems inherent in injecting viscous liquid or solid solutes in Taylor dispersion measurements, the authors developed two impulse response methods to measure diffusion coefficients: the modified Taylor dispersion [13], and the chromatographic impulse response (CIR) method [14,15].

The Taylor dispersion method has also been employed to study diffusion in the near critical region, where some studies report anomalous decreases experimentally [16–19]. We also observed a decrease [20], but could not conclude that these are due to the critical phenomena. Levert Sengers et al. [21] suggested that the Taylor dispersion method is not adequate for measuring D_{12} values in the vicinity of critical density. By performing calculations [22] based on data of Nishiumi et al. [17] in the Taylor dispersion method, we demonstrated that a mixture of solute and carbon dioxide did not attain a supercritical state at most axial positions of the diffusion column; the measurements indicated an anomaly when a relatively large amount of the solute was injected. Clifford and Coleby [23] claimed that the barycentric motion may cause the diffusion anomalies observed in the near critical region in the flowing system. Thus, the critical anomaly in binary diffusion coefficients is not well understood, and the subject is not dealt with in this paper.

In this review, the theoretical background for the Taylor dispersion, modified Taylor dispersion, and CIR method are described. Accuracy, noise elimination technique, correction of apparent binary diffusion coefficient value due to secondary flow effects, and sources of errors are discussed along with the data sources and predictive correlations.

2. Theoretical background of impulse response methods

Fig. 1 shows a schematic diagram of the three impulse response methods: Taylor dispersion, modified Taylor dispersion, and CIR method. The first two methods measure response curves of the solute species diffusing without adsorption in an uncoated capillary column. The last technique is experimentally identical to supercritical fluid chromatography with a polymer-coated open tube column.

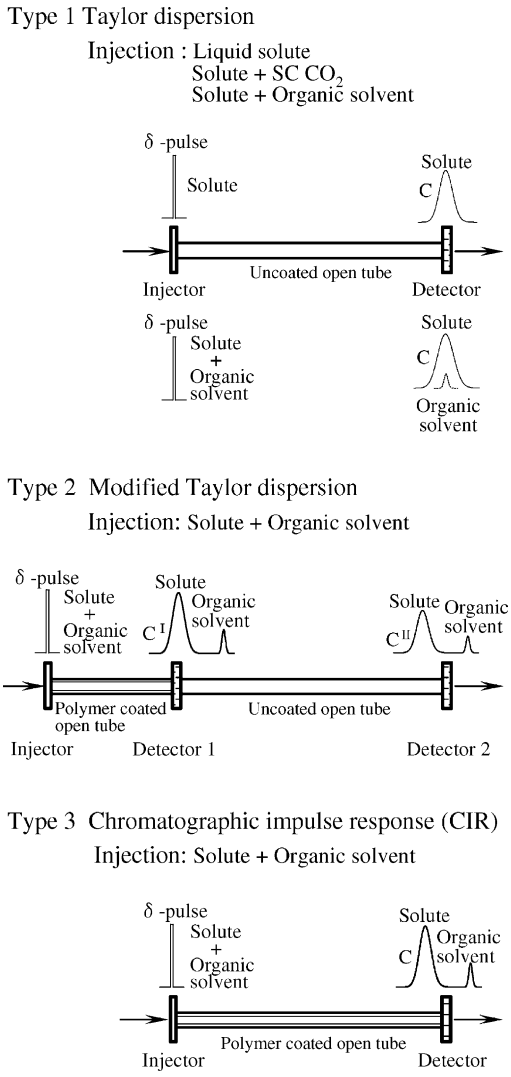

Fig. 1. A schematic diagram of the three types of the impulse response methods.

2.1. Taylor dispersion method

2.1.1. Fundamental equation

When a tracer species is pulse-loaded into a fully developed laminar flow moving in column tubing with a circular cross section, tracer concentration $c(r, x, t)$ is described by Eq. (1) from Taylor [7] and Aris [8]:

$$\frac{\partial c}{\partial t} = D_{12}\left[\frac{1}{r}\cdot\frac{\partial}{\partial r}\cdot\left(r\frac{\partial c}{\partial r}\right)+\frac{\partial^2 c}{\partial x^2}\right] - 2u_a\cdot\left(1-\frac{r^2}{R^2}\right)\cdot\frac{\partial c}{\partial x} \quad (1)$$

where D_{12} is the binary diffusion coefficient of the tracer species, R is tubing radius, u_a is average fluid velocity, t is time, and r and x are radial and axial distances, respectively. Initial and boundary conditions are:

$$c = \frac{m}{\pi R^2}\delta(x) \qquad \text{at } t = 0 \quad (2)$$

$$\frac{\partial c}{\partial r} = 0 \quad \text{at } r = 0 \text{ and } r = R \quad (3)$$

$$c = 0 \qquad \text{at } x = \pm\infty \quad (4)$$

where m is the injected amount of the tracer species. Average concentration per cross-sectional area of tubing is defined by:

$$C(x, t) = \frac{2}{R^2}\int_0^R c(r, x, t)\, r\, \mathrm{d}r \quad (5)$$

Eqs. (1)–(4) can be reduced to [8]:

$$\frac{\partial C_{app}}{\partial t} = K\frac{\partial^2 C_{app}}{\partial x^2} - u_a\frac{\partial C_{app}}{\partial x} \quad (6)$$

$$K = D_{12} + \frac{R^2 u_a^2}{48 D_{12}} \quad (7)$$

$$C_{app} = \frac{m}{\pi R^2}\delta(x) \qquad \text{at } t = 0 \quad (8)$$

$$C_{app} = 0 \quad \text{at } x = \pm\infty \quad (9)$$

The solution of Eqs. (6)–(9) is provided by:

$$C_{app}(x, t) = \left(\frac{m}{\pi R^2}\right)\cdot\frac{1}{\sqrt{4\pi K t}}\cdot\exp\left[-\frac{(x-u_a t)^2}{4Kt}\right] \quad (10)$$

Although C_{app} is not equal to C, the approximation of Eq. (6) has substantially been established as valid [8,24].

The moment method has been used to determine parameter values from the response curve. However, curve fitting in the time domain is more accurate than the moment method. In the curve-fitting method, D_{12} is chosen to minimize the root-mean-square (rms) error ε as defined by:

$$\varepsilon = \left\{\frac{\int_{t_1}^{t_2}[C_{exp}(t) - C_{app}(L, t)]^2\,\mathrm{d}t}{\int_{t_1}^{t_2}[C_{exp}(t)]^2\,\mathrm{d}t}\right\}^{1/2} \quad (11)$$

where L is column length, the period between t_1 and t_2 is selected to provide a measured response curve higher than 10% peak height, and the calculated and measured response curves are compared in the period. Typical response curves measured by injecting acetone in SC carbon dioxide and calculated with assumed parameter values are shown in Fig. 2a [24], together with the fitting errors. A parameter set of the best-fit values is determined using an error contour map as shown in Fig. 2b [24]. The values obtained by the moment method do not agree with the best-fit values determined by the curve-fitting method. As depicted, ε values less than 0.01 indicate a good fit and those less than 0.02 [25] or 0.03 indicate an acceptable fit.

2.1.2. Analytical method of response curve

Response curves were analyzed by graphical peak width measurement, the moment method, or the curve-fitting method. The curve-fitting method is more accurate than the

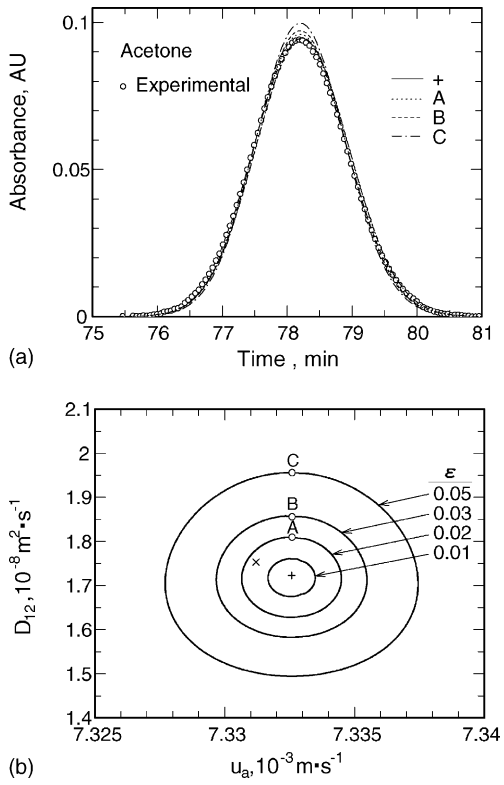

Fig. 2. Parameter determination by the curve-fitting method for acetone in SC CO_2. (a) Response curves observed experimentally (○) at 308.2 K and 10.40 MPa and calculated ((—) best fit; (· · ··) (A) $\varepsilon = 0.02$; (- - -) (B) $\varepsilon = 0.03$; (- · - · -) (C) $\varepsilon = 0.05$) and (b) error contour map for D_{12} vs. fluid velocity u_a, (+) best fit for the curve-fitting method with $\varepsilon = 0.0033$, $u_a = 7.3325 \times 10^{-3}\,m\,s^{-1}$, and $D_{12} = 1.723 \times 10^{-8}\,m^2\,s^{-1}$; (×) moment method with $\varepsilon = 0.015$, $u_a = 7.3312 \times 10^{-3}\,m\,s^{-1}$, and $D_{12} = 1.753 \times 10^{-8}\,m^2\,s^{-1}$). The letters (A–C) correspond to the curves in Fig. 2a. After ref. [24].

moment method [24]. The first two methods are very similar, and for both the binary diffusion coefficients are obtained from variances of the response curves using Eq. (12):

$$\frac{u_a^3}{2L}\sigma^2 = D_{12} + \frac{R^2 u_a^2}{48 D_{12}} \tag{12}$$

where σ^2 is the variance of the response curve. As noted by Wakao and Kaguei [26], the moment method overestimates the errors related to the frontal and tailing portions of the response curves; in particular, in the higher moments.

2.1.3. Initial dispersion of pulse injection

For most measurements, an injected solute is assumed to behave as a delta function, but the dispersion in the input signal, or the variance, is not equal to zero. To avoid the effect of the initial dispersion of the input signal, Dahmen et al. [27] and Umezawa and Nagashima [16] employed Eq. (13) to measure the variances σ^2 in diffusion columns having different lengths or by detecting at two downstream points.

$$\sigma^2 = \sigma^2(L^{II}) - \sigma^2(L^{I}) \tag{13}$$

where L^I and L^{II} designate two distances from the injection point, or lengths of a short and a long column, respectively. However, Catchpole and King [28] have claimed that this can generate errors because the accuracy in variance $\sigma^2(L^I)$ is diminished. If two detectors are placed at the two downstream points, both far from the injection points, to measure signals at the two positions in a single injection with the curve-fitting method, the error can be reduced.

For liquid solutes, the volume of the sample loop of an injector is 0.2–0.5 μL; a larger volume sample loop, e.g., 20 μL, is often used for injecting viscous liquid or solid solutes dissolved in supercritical fluid. According to the theoretical calculations of Arai et al. [29], the initial dispersion of a solute is insignificant, even when the 20-μL sample injector is used. In our experience, using an injector equipped with a 20-μL sample loop results in a response curve that tails.

2.1.4. Wavelength dependency

In general, the wavelength used to obtain a response curve is selected to produce the maximum absorbance intensity. However, this selection may not yield good results. Wavelength dependence on D_{12} values is determined using UV–Vis detection by scanning over a range of wavelengths for a short period of time. Fig. 3 [20] shows the wavelength dependence of (a) absorbance intensity at the maximum peak height of the response curve, (b) detector linearity in terms of normalized absorbance intensity (NAI), which is equal to the maximum absorbance intensity divided by the value of (calculated CO_2 velocity) × (peak area), (c) the rms fitting error ε, and (d) the D_{12} value determined for the response curves, measured for benzene in SC carbon dioxide at 313.15 K and pressures of 11.09, 16.08, and 25.19 MPa by scanning from 220 to 280 nm at a time interval of 1.6 s per scan and a resolution of 1 nm. These studies produced five distinct characteristic peaks at 238, 243, 248, 254, and 260 nm, and two small peaks at 233 and 268 nm. Satisfactory detector linearity should produce constant NAI values. As shown in Fig. 3b, detector linearity failed for the four characteristic peaks, especially at 247, 253, and 259 nm. The rms errors at these three characteristic absorbance wavelengths were higher than those at other wavelengths from 230 to 260 nm, while the values remained less than 0.01. However, NAI values decreased, with a corresponding decrease in D_{12} values. Note that strictly speaking, the wavelengths showing the absorbance peak maxima were slightly different from those showing the maximum rms errors, as well as the NAI value and D_{12} values, as shown in Fig. 3a–d.

For wavelengths of 237–240 nm, and 243–246 nm, the D_{12} values are almost constant and rms errors are low. For wavelengths showing characteristic peaks near 247, 253, and 259 nm, D_{12} values are inaccurate even under good fit conditions, i.e. rms errors <0.01. Thus, the D_{12} values were obtained from the response curves at 239 nm. Fig. 4 [20] shows

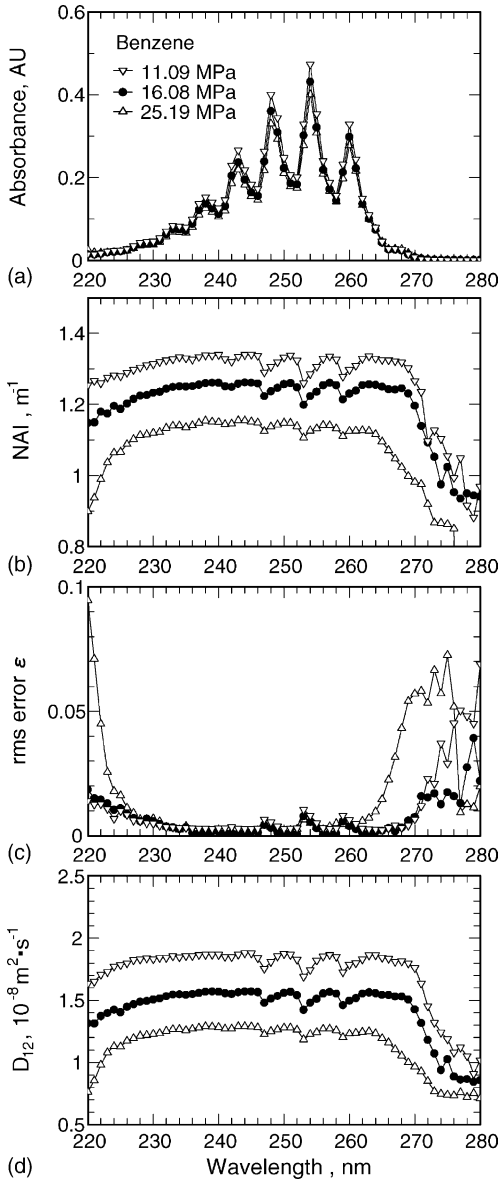

Fig. 3. Wavelength dependence on (a) absorbance intensity for the response curves at the maximum peak heights, (b) normalized absorbance intensity, NAI, (c) rms error ε, and (d) D_{12} values for benzene in SC CO_2, measured at 313.15 K and pressures of 11.09 MPa (▽), 16.08 MPa (●), and 25.19 MPa (△) with 0.2 μL of liquid benzene injected. From ref. [20].

D_{12}/T *versus* carbon dioxide viscosity for the data obtained at 239, 253, and 254 nm. This correlation is valid for various solutes in supercritical carbon dioxide and for the mixture as well as organic solvents, as described in Sections 2.8 and 3.2.2. The data at 239 nm can be represented by a straight line (solid), while the data obtained at 254 and 253 nm are straight lines with values lower by 6.7% (broken-dotted) and 10% (broken), respectively.

Fig. 5 [20] is a comparison of D_{12}/T versus carbon dioxide viscosity for D_{12} data of benzene in SC carbon dioxide at 239 nm [20] with data reported in the literature [3,18,21,30–32], using the Taylor dispersion technique. D_{12}

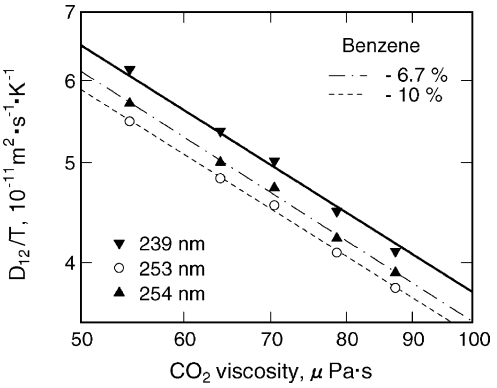

Fig. 4. D_{12}/T vs. CO_2 viscosity for the D_{12} data of benzene in SC CO_2 at 313.15 K and 239 nm (▼), 253 nm (○), and 254 nm (▲). The data at 254 nm and 253 nm are deviated by −6.7% (-·-·-) and by −10% (---), respectively, from the data at 239 nm (—). From ref. [20].

values measured at 253 nm were approximately 10% lower than the data obtained at 239 nm (see Fig. 4), which is consistent with the literature data [21,30,32]. However, the path lengths of the optical cells and/or the wavelength measured were not described in some reports; a main reason for any inconsistency in the D_{12} values could be ascribed to lack of detector linearity caused by measurements taken at a characteristic wavelength such as 253 nm.

2.2. Modified Taylor dispersion method

For solid or highly viscous liquids, injection into the diffusion column is difficult. If a polymer-coated column is installed before an uncoated open capillary column, the solute and the dissolving solvent are chromatographically separated before reaching the inlet of the uncoated column. When the response curve is measured at both inlet

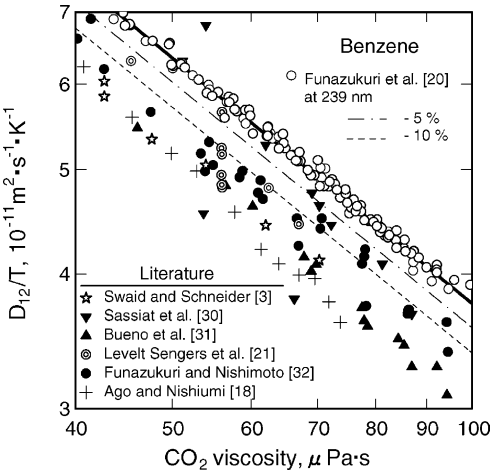

Fig. 5. D_{12}/T vs. CO_2 viscosity for the D_{12} data (○) of benzene in SC CO_2 at 239 nm by Funazukuri et al. [20] and literature data (☆) Swaid and Schneider [3]; (▼) Sassiat et al. [30]; (▲) Bueno et al. [31]; (◎) Levelt Sengers et al. [21]; (●) Funazukuri and Nishimoto [32]; (+) Ago and Nishiumi [18]). From ref. [20].

and outlet of the uncoated diffusion column (see Type 2 in Fig. 1), binary diffusion coefficients are determined from the difference in variance at the two points.

Similar to the original Taylor dispersion method, the cross-sectional average concentration of an injected tracer species is described by Eqs. (6) and (7) in a solvent in laminar flow in tubing with a circular cross section. The initial and boundary conditions for the modified Taylor dispersion method (the input–output response technique) then become:

$$C_{\mathrm{app}} = 0 \qquad \text{at } t = 0 \tag{14}$$

$$C_{\mathrm{app}} = C^{\mathrm{I}}_{\mathrm{exp}}(t) \qquad \text{at } x = 0 \tag{15}$$

The solution for Eqs. (6), (7), (9), (14), and (15) are obtained by the convolution integral in:

$$C^{\mathrm{II}}_{\mathrm{app}}(t) = \int_0^t C^{\mathrm{I}}_{\mathrm{exp}}(\xi)\, f(t-\xi)\, \mathrm{d}\xi \tag{16}$$

where

$$f(t) = \frac{L}{\sqrt{4\pi K t^3}} \cdot \exp\left[\frac{-(L-u_{\mathrm{a}}t)^2}{4Kt}\right] \tag{17}$$

Note that $f(t)$ is the Laplace inversion of the transfer function $F(s)$. As defined by Eq. (18), $F(s)$ is equal to the ratio of the Laplace transformation of the output signal $C^{\mathrm{II}}_{\mathrm{app}}(t)$ to that of the input signal $C^{\mathrm{I}}_{\mathrm{app}}(t)$, where $C^{\mathrm{I}}_{\mathrm{app}}(t)$ and $C^{\mathrm{II}}_{\mathrm{app}}(t)$ are the concentrations at two different downstream points at distance L.

$$F(s) = \frac{\int_0^\infty C^{\mathrm{II}}_{\mathrm{app}}(t)\mathrm{e}^{-st}\,\mathrm{d}t}{\int_0^\infty C^{\mathrm{I}}_{\mathrm{app}}(t)\mathrm{e}^{-st}\,\mathrm{d}t} = \exp\left[\frac{Lu_{\mathrm{a}}(1-\sqrt{1+4Ks/u_{\mathrm{a}}^2})}{2K}\right] \tag{18}$$

The output signal $C^{\mathrm{II}}_{\mathrm{app}}(t)$ can be obtained by Eqs. (16) and (17) with estimated values for u_{a} and D_{12}. The D_{12} value is chosen to minimize the rms fitting error defined in Eq. (11), taking $C^{\mathrm{II}}_{\mathrm{exp}}(t)$ and $C^{\mathrm{II}}_{\mathrm{app}}(t)$ instead of $C_{\mathrm{exp}}(t)$ and $C_{\mathrm{app}}(L,\ t)$, respectively.

Fig. 6 [13] shows (a) the measured input, (b) the measured output response curve, together with calculated value for the best fit, and (c) deviation of the calculated curve from the measured value for α-tocopherol in SC carbon dioxide at 313.15 K and 16.40 MPa. The calculated value for the best fit agrees well with the measured value.

Fig. 7 [13] shows D_{12} values *versus* pressure for phenol, α-tocopherol, and β-carotene at 313.15 K, together with those for these compounds measured by the CIR method, described in Section 2.3, with a poly(ethylene glycol) (PEG) coated capillary column [14]. The values [13] are consistent with those obtained from a PEG coated capillary column. Note that the D_{12} values even for polar compounds such as phenol can be measured accurately by the modified Taylor dispersion using response curves obtained at two points.

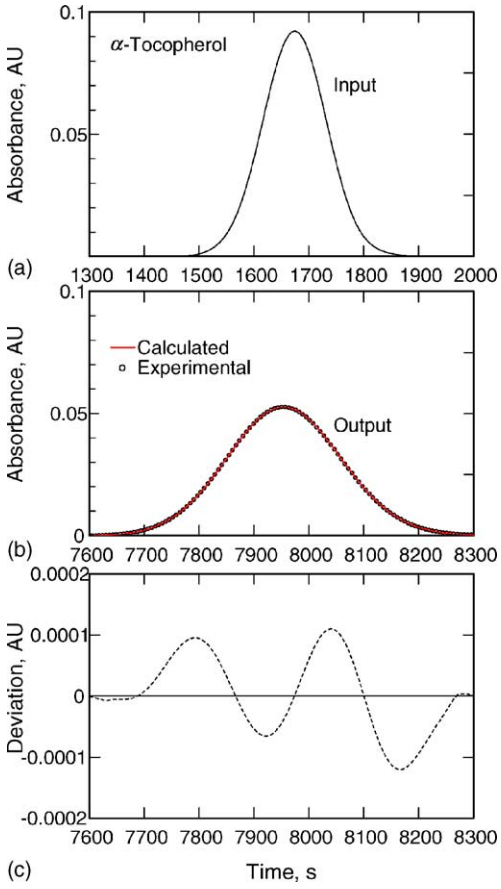

Fig. 6. (a) Input signal measured, (b) output signal calculated (—) for the best fit and measured (○) at 295 nm, and (c) deviation of output signal calculated from that measured for α-tocopherol at 313.15 K and 16.40 MPa for the best fit with $D_{12} = 0.616 \times 10^{-8}\,\mathrm{m^2\,s^{-1}}$ and $\varepsilon = 0.0028$, when α-tocopherol dissolved in hexane was injected. After ref. [13].

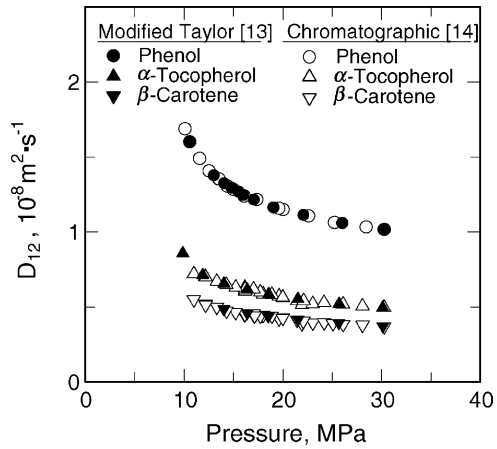

Fig. 7. Comparison of D_{12} values for phenol, α-tocopherol and β-carotene by the modified Taylor dispersion method [13] ((●) phenol; (▲) α-tocopherol; (▼) β-carotene) and the CIR method [14] ((○) phenol; (△) α-tocopherol; (▽) β-carotene). After ref. [13].

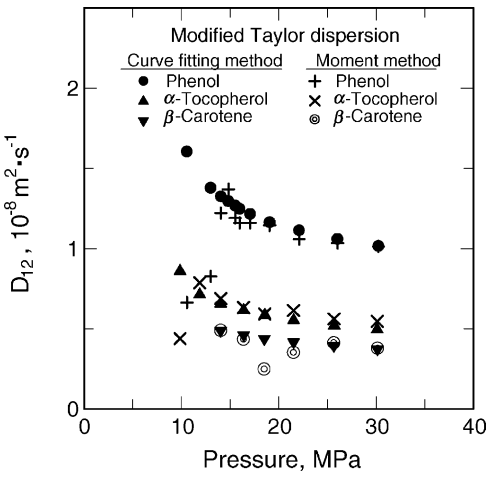

Fig. 8. Comparison of D_{12} values in the modified Taylor dispersion for phenol, α-tocopherol and β-carotene by the curve-fitting method ((●) phenol; (▲) α-tocopherol; (▼) β-carotene) with those by the moment method ((+) phenol; (×) α-tocopherol; (◎) β-carotene). The data for the modified Taylor dispersion measurements are the same as in Fig. 7. After ref. [13].

Fig. 8 [13] is a comparison between the curve-fitting method and moment method for a plot of D_{12} *versus* pressure for the same measurements in the modified Taylor dispersion method shown in Fig. 7. As seen in Taylor dispersion measurements [24], values obtained by the moment method are scattered, whereas those obtained by the curve-fitting method are highly correlated.

2.3. Chromatographic impulse response method

The chromatographic impulse response method is widely performed for measuring physicochemical properties, such as solubility and retention factor for gas chromatography, liquid chromatography, and supercritical fluid chromatography [33–36]. Fig. 1 (Type 3) shows a solution injected into a laminar fluid flowing in an open capillary column whose inner wall was coated with a polymer film. The mixture of solute and solvent chromatographically separate while flowing through the column due to different retention factors, or capacity factor k, defined as the ratio of a solute in the polymer phase to that in the fluid phase.

This method is appropriate for a solid or viscous liquid solute, or a relatively polar compound. The distortion or tailing of response curves for polar compounds, such as phenol, can be minimized by the choice of polymer coating.

The fundamental equation for this system is the Golay's equation [37], and is classified as the telegrapher's equation [38]. Most studies aim to determine thermodynamic properties from peak retention data (the first moments) or to study separation efficiency of chromatographic methods. As mentioned, the curve-fitting method has scarcely been employed because the accuracy of the first moment is acceptable. Binary diffusion coefficients, however, are obtained from the second moment, as determined by Lai and Tan [39], and the values are less reliable. Thus, we provided a theoretical basis to the Gaussian-like approximate solution to the CIR measurements with a curve-fitting method, discussed accuracy, and outlined potential sources of error [15].

When a tracer species is pulse-injected into fully developed laminar flow in a cylindrical tube, tracer concentration can be described by Eq. (1) [14,15], similar to the Taylor dispersion and the modified Taylor dispersion methods. However, boundary conditions are given by:

$$k\frac{\partial c}{\partial t} = -\frac{2D_{12}}{R}\cdot\frac{\partial c}{\partial r} \qquad \text{at } r = R \tag{19}$$

$$\frac{\partial c}{\partial r} = 0 \qquad \text{at } r = 0 \tag{20}$$

$$c = 0 \qquad \text{at } x = \pm\infty \tag{21}$$

where k is the retention factor, assuming that the value is constant, irrespective of axial and radial position in the column and time, but is affected by temperature and pressure. It is also assumed that the tracer species instantly reaches equilibrium between the polymer layer and the supercritical fluid contacting the polymer surface. Practically, k values are determined by measuring peak retention times using Eq. (22), or through the first moment and the solvent flow velocity when the curve-fitting method is not employed.

$$k = \frac{t_{tr} - t_0}{t_0} \tag{22}$$

where t_{tr} and t_0 are the retention times of a tracer (solute) and inert species ($k = 0$), respectively. The initial condition is:

$$c = \frac{m}{\pi R^2}\frac{\delta(x)}{1+k} \qquad \text{at } t = 0 \tag{23}$$

where m is the amount of the tracer species injected.

The Gaussian-like solution often is used as the solution for an impulse response. The average cross-sectional concentration of the column $C(x, t)$ is given by Eq. (5). The approximate solution $C_{app}(x, t)$ for C is:

$$C_{app}(x,t) = \left(\frac{m}{\pi R^2}\right)\cdot\frac{1}{(1+k)\sqrt{4\pi a t}} \times \exp\left\{-\frac{\{x - u_a t/(1+k)\}^2}{4at}\right\} \tag{24}$$

where

$$a = \frac{D_{12}}{1+k} + \frac{1+6k+11k^2}{(1+k)^3}\cdot\frac{R^2 u_a^2}{48 D_{12}} \tag{25}$$

The two parameters of D_{12} and k are determined to minimize rms error ε for the measured (C_{exp}) and calculated (C_{app}) response curves at $x = L$ between t_1 and t_2, as given by Eq. (11), similar to the other two impulse response methods. The fitness of the response curves was considered good when $\varepsilon < 0.01$, and acceptable when $\varepsilon < 0.03$ [15].

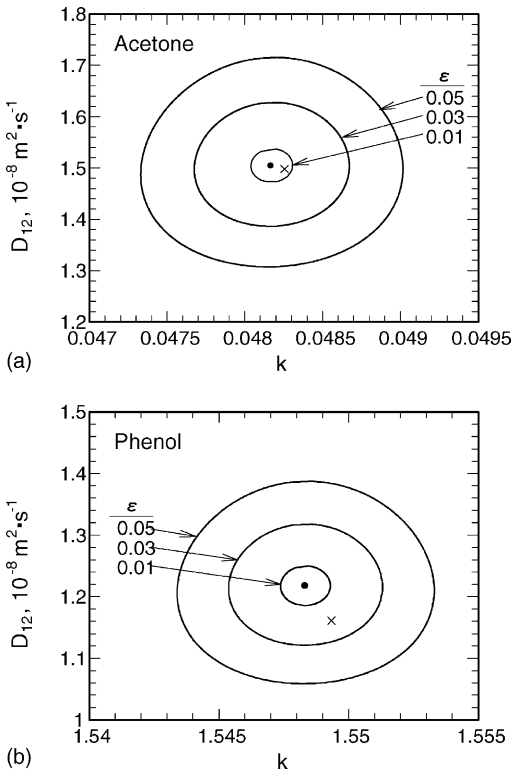

Fig. 9. Error contour maps in the plot of D_{12} vs. k for the data measured at 313.15 K, 17.87 MPa and the velocity $u_{a,exp} = 8.84 \times 10^{-3}$ m s^{-1} for (a) acetone (solvent) and (b) phenol (solute). (●) shows the best-fitted point: $k = 0.0482$ and $D_{12} = 1.51 \times 10^{-8}$ m^2 s^{-1} for acetone and $k = 1.548$ and $D_{12} = 1.22 \times 10^{-8}$ m^2 s^{-1} for phenol; (×) shows that obtained by the moment method. After ref. [15].

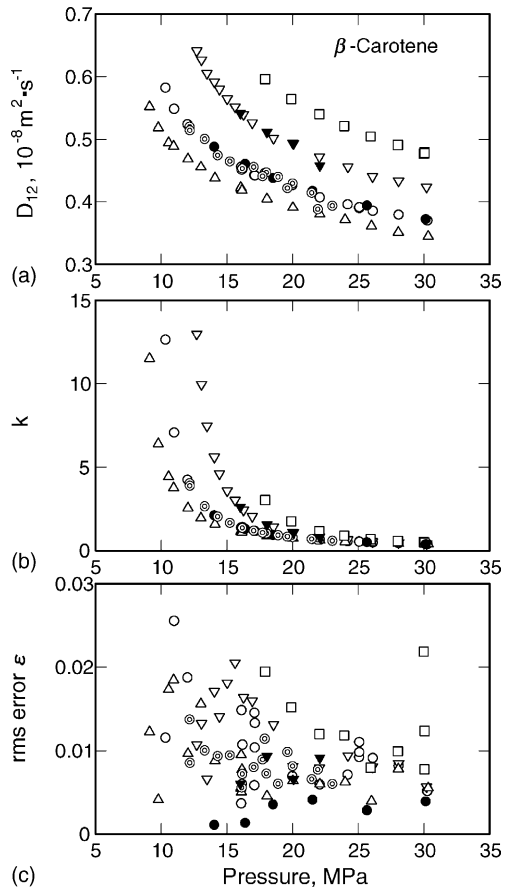

Fig. 10. Pressure dependence on (a) D_{12}, (b) k and (c) fitting error ε for β-carotene in CO_2, (△) 308.15 K, (○) 313.15 K, (▽) 323.15 K, (□) 333.15 K in [40]; (◎) 313.15 K and (▼) 323.15 K in ref. [14], both by the CIR method; (●) 313.15 K in ref. [13] by the modified Taylor dispersion method. After ref. [40].

As shown in Fig. 9 [15], k can be determined directly as a parameter set with D_{12} from the error contour maps for acetone (solvent) and phenol (solute) in the k-D_{12} plane. The best fit of the parameter set of k and D_{12} using the curve-fitting method is not consistent with that obtained by the moment method.

Fig. 10 [40] shows the dependence of pressure on (a) D_{12}, (b) k, and (c) rms fitting error ε for β-carotene in carbon dioxide, together with data obtained by our group [13,14]. D_{12} and k values tended to decrease with increasing pressure, and the data [13,14,40] were consistent. Data obtained by single injections were plotted and yielded good reproducibility [40]. Using this technique, binary diffusion coefficients and retention factors were determined for various compounds [14,15,40–45].

2.4. Sensitivity of parameter values

The accuracy of parameter values strongly depends on pressure [14,20,24,25,40,41]. Although the curve-fitting method provides accuracy in terms of fitting error, sensitivity of the parameter values is not provided directly. The sensitivity of the determined values is estimated by the error contour map. The values of fitting error under supercritical conditions increase with decreasing pressure, especially near the critical region. In CIR measurements, the authors [15] evaluated the parameter sensitivities of k and D_{12} with respect to flow velocity u_a that can be measured directly.

For a small k, i.e., a weak adsorption system:

$$\frac{u_a}{k}\frac{dk}{du_a} \cong \frac{1}{k} \tag{26}$$

$$\frac{u_a}{D_{12}}\frac{dD_{12}}{du_a} \cong 5 \tag{27}$$

For a large k:

$$\frac{u_a}{k}\frac{dk}{du_a} \cong 1 \tag{28}$$

$$\frac{u_a}{D_{12}}\frac{dD_{12}}{du_a} \cong 1 \tag{29}$$

Thus, precise measurement of u_a is required to determine D_{12} for a weak adsorption system in the CIR method because the D_{12} error is five times larger than that of u_a.

Fig. 11 [15] shows the effect of flow velocity on the error contour maps in a k-D_{12} plane for the data in Fig. 9, where I, II, and III designate the error maps at flow velocities $u_{a,exp}$,

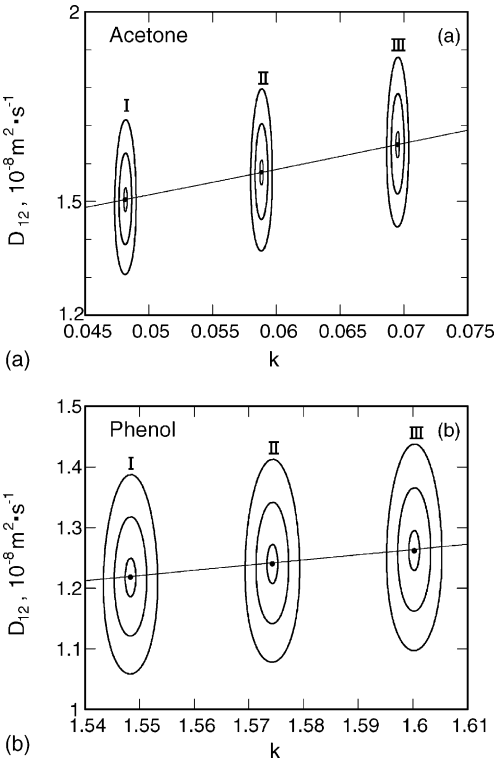

Fig. 11. Error contour maps in the plot of D_{12} vs. k for various u_a values at I: measured $u_{a,exp}$, II: $1.01 \times u_{a,exp}$, and III: $1.02 \times u_{a,exp}$ for the data in Fig. 9. Contours show $\varepsilon = 0.05$, 0.03 and 0.01 from the outer side. From ref. [15].

$1.01u_{a,exp}$, and $1.02u_{a,exp}$, respectively. As depicted, flow velocity directly affects the error map position in the k-D_{12} plane. Thus, fluid velocity must be measured as accurately as possible.

2.5. Improvement of impulse response methods

2.5.1. Noise elimination procedure

The authors [45] applied a noise elimination technique for extracting the response signal from the original response curve having high-frequency noise using a low-pass filter for the impulse response methods. In principle, this method is applicable to any transient response curves, and is effective for response curves showing very weak absorbance intensities if a solute having low solubility and/or at extremely low concentration is injected. Binary diffusion coefficients and retention factors were measured for phenol and β-carotene in the CIR method, and binary diffusion coefficients for acetone were obtained by the Taylor dispersion. As examples of extremely low injected quantities, Fig. 12 [45] plots (a) absorbance at maximum peak height, (b) D_{12}, (c) k, (d) u_a × (peak area), and (e) rms error ε *versus* amount of phenol injected into carbon dioxide flowing in a polymer-coated capillary column at 313.15 K and 17.87 MPa. The values of the binary diffusion coefficient, after noise elimination treatment and analysis by the curve-fitting method, were nearly

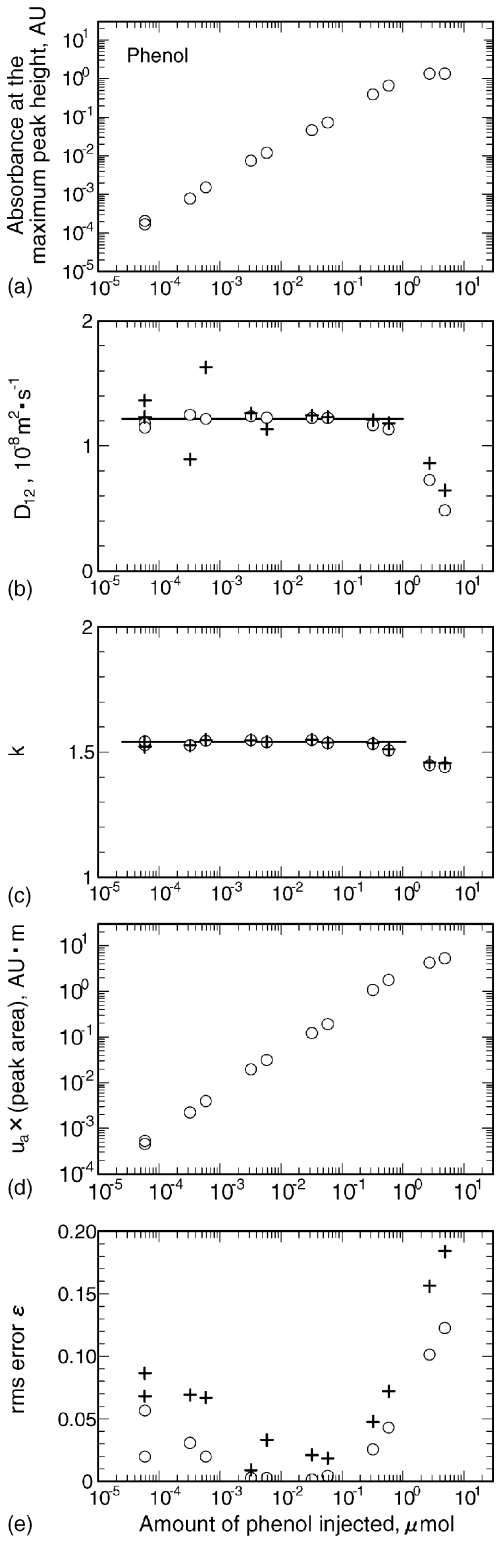

Fig. 12. Effects of the injected amount of phenol on (a) absorbance at the maximum peak height, (b) D_{12}, (c) k, (d) u_a × (peak area), and (e) rms error ε at various injected amounts of phenol dissolved in acetone at 313.15 K and 17.87 MPa, in the CIR method, treated with noise elimination and analyzed by the curve-fitting (○) and the moment method (+). From ref. [45].

constant over a wide range of injected amounts, even at the lowest amount of 6×10^{-5} μmol (1.1×10^{-4} mol m^{-3} at the maximum peak height). This technique also was effective in the Taylor dispersion as well as the CIR method. By combining noise elimination treatment with the curve-fitting method, D_{12} values, obtained from response curves with extremely low absorbance intensities ($=2 \times 10^{-4}$ AU), became coincident with intrinsic values from response curves having normal intensities. Unreliable D_{12} values were obtained from the response curves having lower absorbance intensities by the moment method, even after noise elimination treatment.

2.5.2. Correction of the secondary flow effects

A coiled tube usually is used as a diffusion column, with some exceptions employing a straight capillary column [16,17,47]. The values of diffusion coefficients determined with a coiled tube are affected by secondary flow due to column coiling. This phenomenon has been investigated theoretically by many investigators since Dean [48]. The effect in Taylor dispersion measurements also has been estimated as a function of $De\,Sc^{1/2}$ using the moment method by Alizadeh et al. [49], where De and Sc are the Dean number and Schmidt number, respectively. In most studies, measurements were made for $De\,Sc^{1/2} < 8$ to 10. The effect is less than *ca*. 1%, according to the estimate by Alizadeh et al. The authors derived a correction formula, using a polynomial function of λ, defined as the ratio of tube to coil radius, to correct the values affected by secondary flow. The correction formula is applicable to measurements with an uncoated capillary column in the Taylor dispersion, and a polymer-coated capillary column in the CIR method. Fig. 13 [46] shows the effects of flow velocity in terms of $De\,Sc^{1/2}$ on corrected and directly determined D_{12} values for phenol in carbon dioxide at 313.15 K and 16.10 MPa using CIR measurements. The correction is effective up to a $De\,Sc^{1/2}$ value of *ca*. 20 when the correction formula is expanded in a series of λ^{10}, which provides an effective range of $DeSc^{1/2}$ that is wider than that obtained by Alizadeh et al. [49] using a function of λ^2.

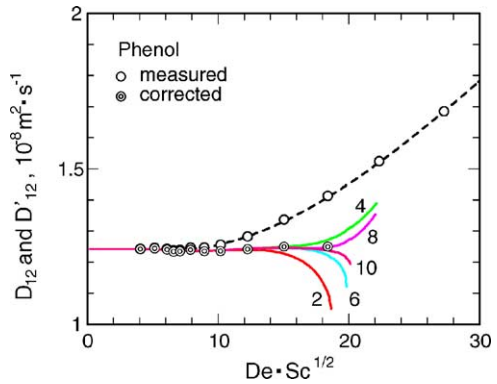

Fig. 13. Correction of the secondary flow effects on the diffusion coefficient, when$k = 1.65$, for phenol in CO_2 at 313.15 K and 16.10 MPa in the CIR measurements; corrected (◎) and measured (○) diffusion coefficients. The letters of 2–10 in the figure indicate the order of λ. After ref. [46].

2.6. Sources of experimental error

Alizadeh et al. [49] estimated the effects of errors due to diffusion tube geometry, dispersion in the monitor cell, and dispersion in the sample injection in terms of the moment. Error sources for Taylor dispersion measurements also were discussed [3,11]. In addition to errors introduced by wavelength dependence, the following experimental errors also are possible.

2.6.1. Diffusion column installation

Natural convection is relatively significant in supercritical phase, as reported by Debenedetti and Reid [50]. To eliminate the effect of gravity or natural convection in supercritical fluids, a diffusion column should be installed horizontally. The authors examined the D_{12} values resulting from horizontal and vertical installation. D_{12} values obtained from vertical installation of an uncoated column with an inner diameter of 0.8 mm were lower than those obtained from a horizontal column [17,32]. Fig. 14 shows plots of the determined values *versus* $DeSc^{1/2}$ for acetone at different solvent flow rates in a 0.817 mm i.d. uncoated column installed horizontally and vertically using the Taylor dispersion, together with the rms error. The effects of secondary flow with vertical and horizontal columns are nearly consistent in Taylor dispersion measurements. However, the trend of the values does not agree with trends reported in the literature. The differences in D_{12} values for naphthalene and in the rms error

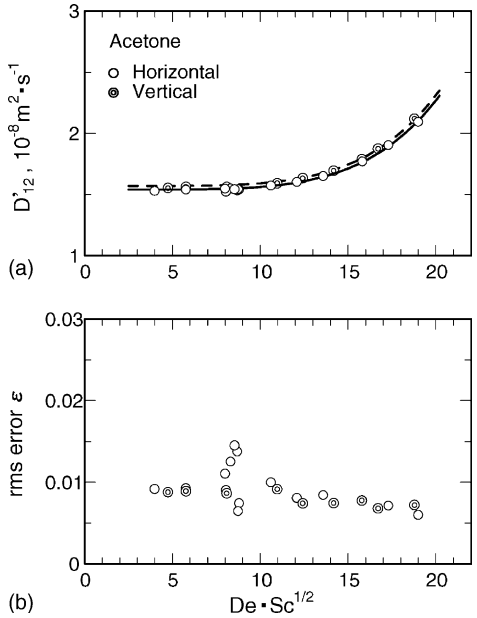

Fig. 14. Effects of the secondary flow due to column installation on (a) apparent binary diffusion coefficients, and (b) rms error ε for acetone in CO_2 at 313.21 K and 16.00 MPa in the Taylor dispersion method with an uncoated capillary column, when the diffusion column was installed horizontally (○) and vertically (◎).

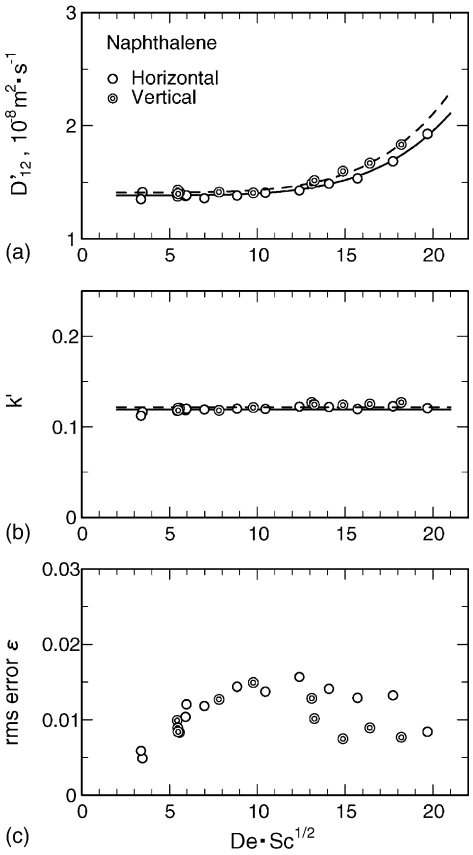

Fig. 15. Effects of the secondary flow due to column installation on (a) apparent binary diffusion coefficients, (b) apparent retention factors, and (c) rms error ε for naphthalene in CO_2 at 313.21 K and 11.00 MPa by the CIR method with a polymer-coated capillary column, when the diffusion column was installed horizontally (○) and vertically (◎).

between the two installations are small, except for higher $DeSc^{1/2}$ values using the CIR method with a polymer-coated column ($2R = 0.515$ mm), as shown in Fig. 15. However, k' values are barely influenced by installation orientation in polymer-coated columns. Despite a lack of explanation for the effects, a horizontal column installation is recommended.

2.6.2. Effect of weak adsorption of solute on the inner wall of uncoated diffusion column

The authors [15] derived Eq. (30) from the Gaussian-like approximate solution, Eq. (24), of the CIR measurements.

$$\frac{D_{12} - D_{12,0}}{D_{12}} \cong \frac{k(5 + 11k)}{1 + 6k + 11k^2} \tag{30}$$

where D_{12} and $D_{12,0}$ are the determined values assuming $k \neq 0$ and $k = 0$, respectively. If $k = 0.1$ and 0.01, error was 36 and 5%, respectively. The estimation of k values is difficult for an uncoated capillary column. Unfortunately, the assumption of $k = 0$, even for weak polar compounds, leads to significant error in the determined value.

2.6.3. Initial condition of Lai and Tan

Lai and Tan [39] employed an initial condition of Eq. (31) for CIR measurements.

$$C_{\text{app}} = \frac{m}{\pi R^2}\frac{\delta(t)}{u_a} \quad \text{at } x = 0 \tag{31}$$

We [15] examined the difference resulting from initial conditions produced by Eqs. (23) and (31). The results were not influenced by the initial conditions.

2.6.4. Effect of surface diffusion due to concentration gradient

The contribution of diffusion of the adsorbed species on the surface of a polymer film coated on the inner column wall due to a concentration gradient was examined [15]. Surface diffusion can be expressed by:

$$k\frac{\partial c}{\partial t} = kD_s\frac{\partial^2 c}{\partial x^2} - \frac{2D_{12}}{R}\frac{\partial c}{\partial r} \quad \text{at } r = R \tag{32}$$

where D_s is the surface diffusion coefficient based on concentration gradient of the adsorbate. Under the conditions set by Eq. (32), a in Eq. (25) should be replaced by a^* in:

$$a^* = \frac{D_{12} + kD_s}{1 + k} + \frac{1 + 6k + 11k^2}{(1 + k)^3}\frac{R^2 u_a^2}{48\, D_{12}} \tag{33}$$

Because D_s can be considered to be smaller than D_{12}, making the second term is dominant in Eq. (33). Thus, surface diffusion effects do not need to be considered for CIR measurements.

2.6.5. Effect of organic solvent when injecting solute dissolved in organic solvent

Solid or viscous liquid solutes dissolved in an organic solvent without UV–Vis absorption such as hexane [33,51,52], and isooctane [30] can be injected into an uncoated diffusion column. While absorbance of the solvent was negligible, mean residence times of the solvent and solute are nearly identical unless the molecular weights or binary diffusion coefficients are significantly different. Solvent effects have not been fully elucidated, although the data indicate that solutes dissolved in an organic solvent yield results consistent with those in the absence of organic solvents. To examine the organic solvent effects in CIR measurements, several pulses of neat acetone were repeatedly injected immediately after the pulse of the solute dissolved in acetone [15]. Fig. 16a [15] shows the response curve measured at the column exit upon injection of three impulses of acetone. Note that the first peak (#0) of acetone appearing at *ca.* 1800 s corresponds to the pulse of phenol solution. Fig. 16b and c show k and D_{12} values obtained from the response curves passed by several pulses of acetone. Since k and D_{12} do not depend on the number of additional pulses, it can be concluded that the diffusion of phenol in the column is not affected by the solvent.

2.6.6. Column radius

An accurate measurement of the diameter of the diffusion column is essential for determination of binary diffusion coefficients. Under supercritical or liquid conditions, the second terms are dominant for K or a values in Eqs. (7) or

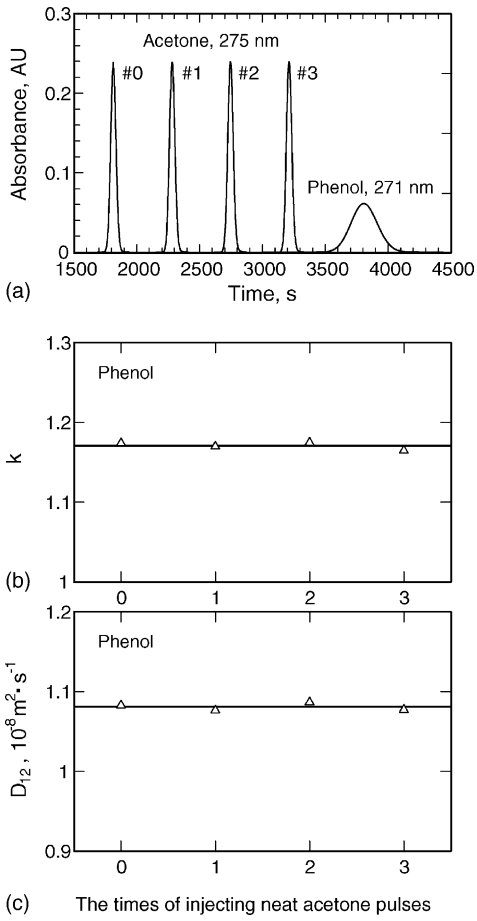

Fig. 16. Effects of the solvent. (a) Response curves (chromatogram) for three acetone pulses after loading a pulse of acetone solution of phenol, measured at 313.15 K, and 25.09 MPa, and (b) k and (c) D_{12} for phenol vs. the times of injecting the acetone impulses, where zero in the x-axis designates the injection of phenol dissolved in acetone. From ref. [15].

(25), respectively. Thus, an error in radius ΔR directly influences the determined D_{12} value. For the Taylor dispersion method, when K and u_a are constant:

$$\frac{R}{D_{12}}\frac{\mathrm{d}D_{12}}{\mathrm{d}R} \cong 2 \tag{34}$$

Thus, the relative D_{12} error, i.e., $\Delta D_{12}/D_{12}$, is two times larger than that of R. For the CIR method, if a: constant, $u_a/(1+k)$: constant, and R^2u_a: constant, then:

$$\frac{R}{k}\cdot\frac{\mathrm{d}k}{\mathrm{d}R} = -\frac{2(1+k)}{k} \tag{35}$$

$$\frac{R}{D_{12}}\frac{\mathrm{d}\,D_{12}}{\mathrm{d}\,R} \cong -\frac{8(1+4k)}{1+6k+11k^2} \tag{36}$$

when k is small, the relative D_{12} error is almost eight times larger than that of R. Consequently, a more accurate measure of R is required for the CIR method than for the Taylor dispersion method. In contrast, when k is large, the relative D_{12} error is small, which results in an advantage of the CIR method over the Taylor dispersion method. For example, when $k > 1.1$, $\Delta D_{12}/D_{12} < 2\Delta R/R$ and the value of $\Delta D_{12}/D_{12}$ approaches zero as k becomes infinity.

We examined the accuracy of the tube diameter in two ways: measured by an X-ray microanalyzer and obtained from the mean residence time of a tracer injected to a laminar flow of an organic solvent at atmospheric pressure [14,24]. In the Taylor dispersion method, Alizadeh et al. [49] evaluated the effect of the axial deviation of the diffusion column diameter, the dispersion in the detector cell, and the effect of the short column.

2.7. Determination of partial molar volume

Determining partial molar volumes (PMV) of a solute at infinite dilution in supercritical fluid mixtures is difficult because accurate PVT data of the mixtures and pure components are required [53]. However, the value can be determined from the retention factor using the CIR method with a polymer-coated capillary or a packed bed composed of polymer-coated porous particles. The retention factor k is expressed by:

$$\left(\frac{\partial(\ln k)}{\partial(\ln \rho)}\right)_T = \frac{v_m^\infty - v_s^\infty}{R_g T \beta_T} - 1 \tag{37}$$

where v_m^∞ and v_s^∞ are the solute PMV for the mobile phase and the stationary phase, respectively, and ρ is fluid density, R_g is gas constant, and β_T is isothermal compressibility of the fluid.

PMV values at infinite dilution of various solutes such as α-tocopherol [40], β-carotene [40], ubiquinone CoQ10 [41], and unsaturated fatty acids [42,43] were determined using the CIR method, assuming v_s^∞ was negligible compared with v_m^∞. This assumption may be valid in the near critical region. If v_s^∞ is measured separately or estimated accurately, a more reliable v_m^∞ value is obtained.

As an example, the k values of α-tocopherol are plotted against carbon dioxide density in Fig. 17, and the determined PMV values are shown in Fig. 18, along with those predicted with the modified Redlich–Kwong–Soave equation of state with interaction parameters k_{ij} determined by Crevatin et al.

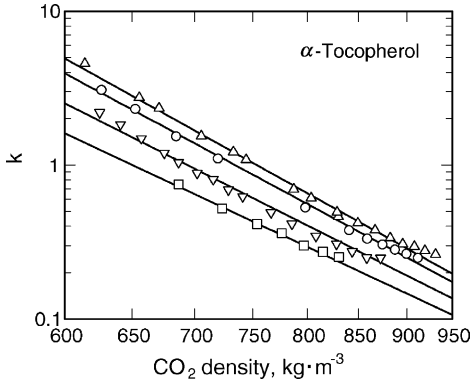

Fig. 17. Retention factor k vs. CO_2 density for α-tocopherol. The key is the same as in Fig. 10. From ref. [40].

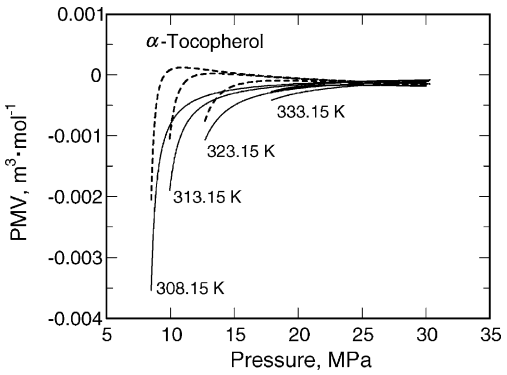

Fig. 18. Partial molar volume for α-tocopherol in CO_2 for (—) obtained from the k values; (- - -) predicted by the modified Redlich–Kwong–Soave equation of state with k_{ij} values determined by Crevatin et al. [54]. From ref. [40].

[54]. The determined PMV values and those predicted by the equation of state were in agreement.

2.8. Measurements of pseudo binary diffusion coefficients

In the design of reactors for supercritical extraction, chromatography, and distillation, pseudo binary diffusion coefficient D_{1m} of a solute in supercritical fluids containing small amounts of an entrainer or a modifier are required. The pseudo binary diffusion coefficients have been measured by the Taylor dispersion method [30,55–63]. The design of the experimental apparatus for a mixture of solvents is essentially identical. Funazukuri and Ishiwata [59] measured the pseudo binary diffusion coefficient D_{1m} of linoleic acid methyl ester, indole, and Vitamin K_3 at 313 K in a mixture of carbon dioxide and hexane over the entire range of hexane mole fractions from zero to 1. The D_{1m} values decrease with increasing hexane mole fraction, as shown in Fig. 19 [59]. Eq. (38), called Blanc's equation, and the D_{1m}-viscosity correlation expressed as Eq. (39) are more representative of conventional correlations [59].

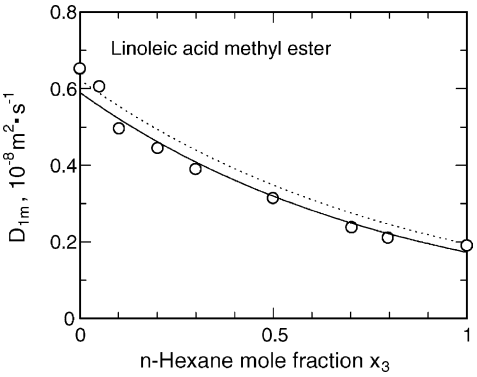

Fig. 19. Comparison of diffusion coefficients D_{1m} for linoleic acid methyl ester in mixed solvent of CO_2 and hexane at various compositions at 313.2 K and 16.0 MPa, predicted by correlations in Eq. (38) (—) and Eq. (39) (- - - -), together with measured D_{1m} values (○). After ref. [59].

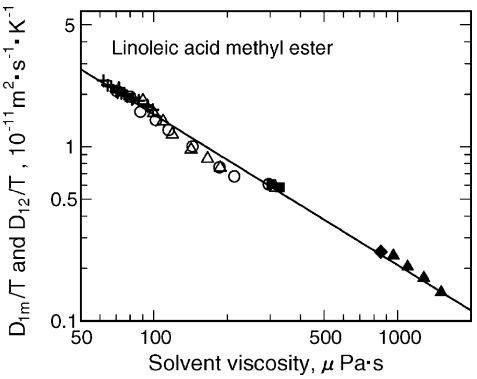

Fig. 20. D_{1m}/T and D_{12}/T vs. solvent viscosity at 313.2 K, and total pressure of 16.0 MPa (△) and 25.0 MPa (○) for linoleic acid methyl ester in mixture of carbon dioxide and hexane, together with binary diffusion coefficient D_{12} in supercritical CO_2 (+) [51], and D_{12} in organic solvents [64]; *n*-hexane (■), *n*-dodecane (▲), and cyclohexane (◆). After ref. [59].

$$D_{1m} = \frac{1}{x_2/D_{12} + x_3/D_{13}} \tag{38}$$

where x_2, and x_3 are mole fractions of carbon dioxide and hexane, respectively, and D_{12} and D_{13} are binary diffusion coefficients of a solute in carbon dioxide and in hexane, respectively, at the same temperature and pressure.

$$\frac{D}{T} = \alpha\eta^{\beta} \tag{39}$$

where D is binary diffusion coefficient D_{12} for diffusion of a solute in pure solvent or pseudo binary diffusion coefficient D_{1m} for diffusion of a solute in mixed solvent, correspondingly η is viscosity of a pure solvent or a mixed solvent, respectively, and α and β are constants, whose values are specific to the solute and the solvent [32,64]. However, Eq. (39) with a single set of values of α and β is valid for a specific solute in supercritical carbon dioxide and organic solvents, as shown in Fig. 20 [59]. Note that the D_{1m} values in a mixture solvent of carbon dioxide and hexane deviated because of uncertainty in the estimated viscosity of the mixture by the method of Chung et al. (described in ref. [65]) with an accuracy of 8–9% claimed [65] for the method.

3. Measured binary and pseudo binary diffusion coefficient data and the correlations

3.1. Data sources

Many studies have reported data on binary diffusion coefficients obtained using a variety of methods, including:

(1) In carbon dioxide by the Taylor dispersion method [3,16–21,24,25,27,28,30–33,47,51,52,55,56,58,60,64,66–85].
(2) In carbon dioxide by the modified Taylor dispersion method [13].

(3) In carbon dioxide by the chromatographic impulse response (CIR) method [14,15,39–45].
(4) In other supercritical fluids by the Taylor dispersion method [86–90].
(5) In a dense fluid mixture by the Taylor dispersion method [30,55–63].
(6) In dense carbon dioxide with micelle-forming surfactant and water [85]
(7) From solid dissolution rates in supercritical fluids [1,2,91,92].
(8) From solid dissolution rates in supercritical fluids laminarly flowing in a rectangular channel [50].
(9) Of a viscous liquid (methyl oleate) from dissolution rates in a parallel plate channel, in which supercritical carbon dioxide was continuously flowing over a porous plate placed on the surface of the liquid sample [93].
(10) Of a solid or viscous liquid by the capillary evaporation technique [28,94–96].
(11) In gaseous phases of a single component and mixtures from ambient to 250 atm (1 atm = 101325 Pa) with a diaphragm cell chamber using radioactive tracers [97–101].
(12) By a light scattering (photon correlation) method in mixture [102].
(13) By a nuclear magnetic resonance (NMR) method [103].

3.2. Correlations

While predictive correlations have been proposed by many investigators, the validity of these predictions is supported by a limited amount of data. Although the accuracy of all of the correlations has not been confirmed, two correlations are effective for compounds over a wide range of molecular mass, as shown in Table 1, which lists data obtained with impulse response methods such as the Taylor dispersion [20,24,25,45], modified Taylor dispersion [13], and CIR method [14,15,40–45].

3.2.1. Schmidt number correlation

Funazukuri and Wakao [104] proposed the Schmidt number correlation for predicting binary diffusion coefficients as well as self-diffusion coefficients from low- to high-pressure regions as:

$$Sc^{+} = \frac{Sc}{Sc^{*}} = 1 + \exp\left[\sum_{i=0}^{5} a_i \left(\frac{v_0}{v}\right)^i\right] \tag{40}$$

where

$$Sc^{*} = \frac{5}{6}\left[\frac{\sigma_1+\sigma_2}{2\sigma_2}\right]^2\left[\frac{2M_1}{M_1+M_2}\right]^{1/2} \quad \text{for binary diffusion} \tag{41}$$

and

$$Sc^{*} = \frac{5}{6} \quad \text{for self-diffusion} \tag{42}$$

The coefficients a_i are listed in Table 2. Sc and Sc^{*} are Schmidt numbers at high pressure and atmospheric pressure, respectively, at the same temperature, v is molar volume of the solvent, v_0 is the hard-sphere closest-packed volume of solvent molecules, and σ_1 and σ_2 are hard-sphere diameters for the solute and solvent, respectively. The v_0 values for carbon dioxide can be obtained by the polynomial function of temperature, proposed by Funazukuri et al. [52]:

$$v_0 = \frac{1}{1.384}\left(\sum_{i=0}^{4} c_i T^i\right) \tag{43}$$

where the constants c_i are listed in Table 3. When σ_1 is not available, the following assumption is made:

$$\frac{\sigma_1}{\sigma_2} = \frac{\sigma_{vw,1}}{\sigma_{vw,2}} \tag{44}$$

where $\sigma_{vw,1}$ and $\sigma_{vw,2}$ are van der Waals diameters of solute and solvent molecules, respectively, obtained from the method described by Bondi [105].

Values of average absolute deviation (AAD%) for compounds are listed in Table 1. For compounds having low molecular weights, the binary diffusion coefficients were accurately predicted using the van der Waals diameter as the molecular diameter. For this case, Eq. (40) involves no adjustable parameter. For compounds having large molecular weights, e.g., α-tocopherol, the accuracy in the prediction using van der Waals diameter (σ_{vw} = 0.967 nm) decreases as shown in Fig. 21a. When the molecular diameter (σ = 0.888 nm) is chosen as an adjustable parameter listed in Table 1, the prediction improves (see Fig. 21b).

For data showing the critical anomalous decrease, deviations from background values directly corresponded to the deviations from the correlation, as shown for benzene in carbon dioxide in Fig. 22.

3.2.2. D/T versus viscosity correlation

Eq. (39) is valid for D_{12} data in supercritical fluids and various organic solvents under pressure, and D_{1m} data in dense mixtures of carbon dioxide and hexane. It is not theoretically derived, but empirically obtained. The constants α and β are specific to the system and are related to the solvent and a solute. No correlation to predict α and β has been developed. However, it is interesting that Eq. (39) with a single set of α and β values represents the D_{12} and D_{1m} values for a specific solute in various solvents: supercritical carbon dioxide, mixtures of carbon dioxide and hexane over the entire range of mole fraction at different pressures, and various organic solvents, as shown in Fig. 20.

The values of α and β for each solute are listed in Table 1, together with the effective range of temperature and pressure, where the values α and β were assumed to be independent of temperature. Note that α and β are affected slightly by temperature [14,41]. Moreover, the constants in Eq. (39) were determined with data that included values showing decreases near the critical conditions.

Table 1
Solutes whose binary diffusion coefficients D_{12} were measured by the transient response methods

Solute		M	Method	T (K)	P (MPa)	Number of data	Schmidt number correlation				D_{12}/T-CO_2 viscosity correlation			Reference
							σ_{vw} (nm)	AAD (%)	σ (nm)	AAD (%)	α	β	AAD (%)	
2-Propanone	C_3H_6O	58.1	CIR	313.15	8.2–34.8	67								[14]
			CIR	313.15	11.6–28.6	14								[15]
			T	308.2–313.2	7.9–40.1	121	0.498	6.3	0.511	5.7	1.594×10^{-14}	−0.843	4.7	[24]
			T	308.15–328.15	11.1–34.6	42								[25]
			T	313.21	16.0	1								[45]
2-Butanone	C_4H_8O	72.1	T	308.15–328.15	8.3–34.5	38	0.539	2.2	0.537	2.2	2.081×10^{-14}	−0.803	1.5	[25]
2-Pentanone	$C_5H_{10}O$	86.1	T	308.15–314.50	7.6–29.3	24	0.574	4.4	0.568	4.2	2.704×10^{-14}	−0.767	2.8	[25]
3-Pentanone	$C_5H_{10}O$	86.1	T	308.15–328.15	8.7–34.6	39	0.574	3.5	0.559	2.1	1.460×10^{-14}	−0.832	1.2	[25]
Benzene	C_6H_6	78.1	T	308.15–328.15	6.0–34.5	176	0.535	11.9	0.504	9.9	3.700×10^{-14}	−0.751	5.5	[20]
Phenol	C_6H_6O	94.1	MT	313.15	10.6–30.3	11								[13]
			CIR	308.15–328.15	8.7–30.3	64	0.555	4.4	0.571	3.5	2.272×10^{-14}	−0.783	2.4	[14]
			CIR	313.15	11.6–28.6	14								[15]
			CIR	313.15	17.87	1								[45]
Vitamin K_3	$C_{11}H_8O_2$	172.1	MT	313.15	9.0–30.0	17	0.660	3.6	0.664	3.6	2.580×10^{-14}	−0.744	0.5	[13]
α-Tocopherol	$C_{29}H_{50}O_2$	430.7	MT	313.15	9.9–30.1	8								[13]
			CSR	313.15–323.15	12.2–23.1	21	0.967	11.4	0.888	2.1	9.805×10^{-15}	−0.796	1.4	[14]
			CSR	308.15–333.15	8.5–30.3	53								[40]
β-Carotene	$C_{40}H_{56}$	536.9	MT	313.15	14.1–30.2	6								[13]
			CIR	313.15–323.15	12.2–23.0	21	1.045	5.8	1.091	2.6	1.140×10^{-14}	−0.749	1.6	[14]
			CIR	308.15–333.15	9.1–30.3	63								[40]
			CIR	313.15	16.14	1								[45]
Ubiquinone CoQ10	$C_{59}H_{90}O_4$	863.4	MT	313.15	12.1–30.2	9	1.276	17.1	1.126	3.7	9.261×10^{-15}	−0.764	3.2	[13]
			CIR	308.15–333.15	8.5–30.2	71								[41]
α-Linolenic acid	$C_{18}H_{30}O_2$	278.4	CIR	308.15–343.15	8.5–30.1	56	0.838	2.8	0.848	2.3	1.215×10^{-14}	−0.783	1.7	[42]
Linoleic acid	$C_{18}H_{32}O_2$	280.4	CIR	308.15–343.15	8.5–30.3	71	0.843	3.7	0.854	3.4	2.513×10^{-14}	−0.706	1.9	[43]
Oleic acid	$C_{18}H_{34}O_2$	282.5	CIR	313.21	9.5–30.1	19	0.848	4.6	0.863	3.8	2.150×10^{-14}	−0.720	1.0	[44]
Elaidic acid	$C_{18}H_{34}O_2$	282.5	CIR	313.21	11.0	1	0.848	–	–	–	–	–	–	[44]
Linoleic acid ME	$C_{19}H_{34}O_2$	294.5	CIR	313.21	11.0	1	0.858	–	–	–	–	–	–	[44]
Oleic acid ME	$C_{19}H_{36}O_2$	296.5	CIR	313.21	8.0–11.0	19	0.863	10.1	0.926	4.9	1.566×10^{-14}	−0.755	3.0	[44]
Elaidic acid ME	$C_{19}H_{36}O_2$	296.5	CIR	313.21	11.0	1	0.863	–	–	–	–	–	–	[44]
EPA	$C_{20}H_{30}O_2$	302.5	CIR	308.15–343.15	8.7–30.2	55	0.858	4.8	0.891	1.6	1.079×10^{-14}	−0.788	0.7	[42]
Arachidonic acid	$C_{20}H_{32}O_2$	304.5	CIR	308.15–343.15	9.5–30.5	75	0.863	4.8	0.891	3.1	1.949×10^{-14}	−0.727	1.3	[43]
Linolenic acid EE	$C_{20}H_{34}O_2$	306.5	CIR	313.21	11.0	1	0.868	–	–	–	–	–	–	[44]
Linoleic acid EE	$C_{20}H_{36}O_2$	308.5	CIR	313.21	11.0	1	0.873	–	–	–	–	–	–	[44]
Oleic acid EE	$C_{20}H_{38}O_2$	310.5	CIR	313.21	8.6–11.0	5	0.878	7.0	0.922	2.7	4.194×10^{-14}	−0.657	2.6	[44]
Elaidic acid EE	$C_{20}H_{38}O_2$	310.5	CIR	313.21	11.0	1	0.878	–	–	–	–	–	–	[44]
DHA	$C_{22}H_{32}O_2$	328.5	CIR	308.15–343.15	9.3–30.1	63	0.881	6.8	0.927	1.3	8.169×10^{-15}	−0.811	0.7	[42]
DHA ME	$C_{23}H_{34}O_2$	342.5	CIR	313.21	11.0	1	0.895	–	–	–	–	–	–	[44]
DHA EE	$C_{24}H_{36}O_2$	356.5	CIR	313.21	11.0	1	0.909	–	–	–	–	–	–	[44]
Monoolein	$C_{21}H_{40}O_4$	356.5	CIR	313.21	10.0–25.0	11	0.901	4.4	0.933	2.2	1.406×10^{-14}	−0.755	0.8	[44]
Dilinolein	$C_{39}H_{68}O_5$	617.0	CIR	313.21	11.0	1	1.088	–	–	–	–	–	–	[44]
Diolein	$C_{39}H_{72}O_5$	621.0	CIR	313.21	10.0–25.0	9	1.094	6.7	1.039	2.0	1.032×10^{-14}	−0.767	1.1	[44]
Trilinolenin	$C_{57}H_{92}O_6$	873.4	CIR	313.21	11.0	1	1.221	–	–	–	–	–	–	[44]
Trilinolein	$C_{57}H_{98}O_6$	879.4	CIR	313.21	11.0	1	1.228	–	–	–	–	–	–	[44]
Triolein	$C_{57}H_{104}O_6$	885.4	CIR	313.21	9.1–14.0	10	1.236	9.0	1.150	2.0	1.986×10^{-14}	−0.685	0.8	[44]
Trielaidin	$C_{57}H_{104}O_6$	885.4	CIR	313.21	11.0	1	1.236	–	–	–	–	–	–	[44]
Triarachidonin	$C_{63}H_{98}O_6$	951.5	CIR	313.21	11.0	1	1.256	–	–	–	–	–	–	[44]

ME: methyl ester, EPA: *cis*-5,8,11,14,17-eicosapentaenoic acid, EE: ethyl ester, DHA: *cis*-4,7,10,13,16,19-docosahexaenoic acid, T: Taylor dispersion, MT: modified Taylor dispersion, CIR: chromatographic impulse response.

Table 1
Constants in correlation of Schmidt number with solvent molar volume in Eq. (40)

i	a_i
0	−4.92519817
1	5.45529385×10^{1}
2	$-2.45231443 \times 10^{2}$
3	6.07893924×10^{2}
4	$-7.08884016 \times 10^{2}$
5	3.29611433×10^{2}

Table 2
Constants in correlation of effective hard-sphere packed volume in Eq. (43)

i	c_i
0	4.452×10^{-5}
1	-1.152×10^{-7}
2	2.749×10^{-10}
3	-3.073×10^{-13}
4	1.290×10^{-16}

3.3. Effects of degree of unsaturation for lipids

Binary diffusion coefficients for various compounds in supercritical carbon dioxide decrease with increasing molecular size or molecular weight, as measured by the CIR method with a polymer-coated capillary column and shown in Fig. 23a [44], while retention factors are not correlated with molecular weight, as shown in Fig. 23b. However, the values are secondarily affected by the polarity of the solute for lipids having identical carbon numbers but a different number of double bonds. Fig. 24 plots D_{12} value versus number of C–C double bonds at 313.21 K and 11 MPa for C_{18} and C_{20} unsaturated fatty acids, methyl/ethyl esters and triglycerides [44]. The D_{12} values decreased with increasing number of double bonds for C_{18} methyl and ethyl esters, and the triglycerides. In contrast, C_{18} and C_{20} acids showed the opposite trend. This may partly result from the stronger effect of a carboxyl group than the effect exerted by multiple

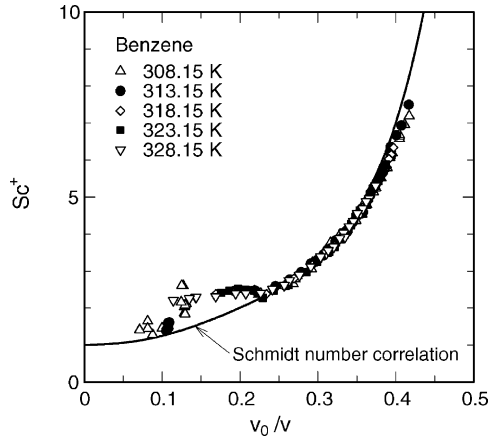

Fig. 22. Plot of Schmidt number correlation for benzene ((△) 308.15 K, (●) 313.15 K, (◇) 318.15 K, (■) 323.15 K, (▽) 328.15 K). From ref. [20].

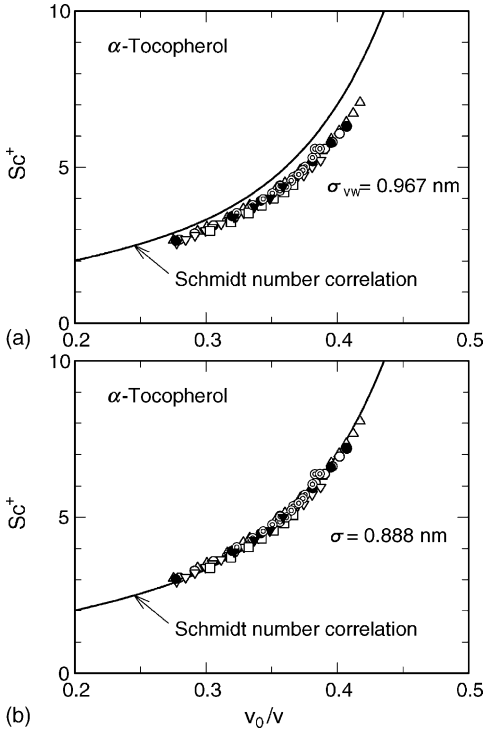

Fig. 21. Schmidt number correlation for α-tocopherol [13,14,40]. (a) van der Waals diameter ($\sigma_{vw} = 0.967$ nm); and (b) $\sigma = 0.888$ nm. The key is the same as in Fig. 10; (—) represented by the correlation. After ref. [40].

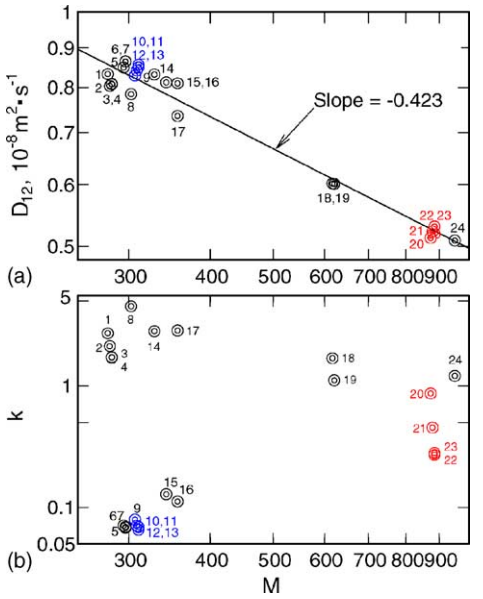

Fig. 23. (a) D_{12} vs. molecular weight M, and (b) k vs. M for lipids and their derivatives. (1) α-linolenic acid; (2) linoleic acid; (3) oleic acid; (4) elaidic acid; (5) linoleic acid methyl ester (ME); (6) oleic acid ME; (7) elaidic acid ME; (8) EPA; (9) arachidonic acid; (10) linolenic acid ethyl ester (EE); (11) linoleic acid EE; (12) oleic acid EE; (13) elaidic acid EE; (14) DHA; (15) DHA ME; (16) DHA EE; (17) monoolein; (18) dilinolein; (19) diolein; (20) trilinolenin; (21) trilinolein; (22) triolein; (23) trielaidin; (24) triarachidonin. After ref. [44].

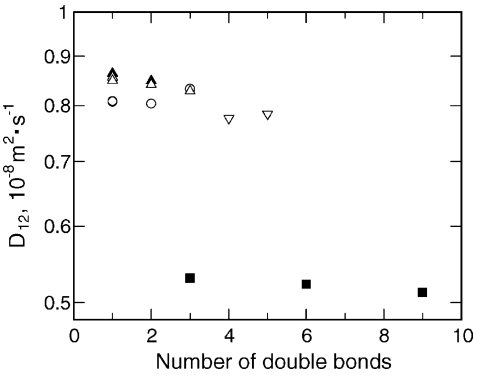

Fig. 24. D_{12} value vs. number of C–C double bond at 313.21 K and 11 MPa for some lipid compounds: C_{18} acid (○), C_{18} methyl ester (▲), C_{18} ethyl ester (△), triglyceride (■), C_{20} acid (▽). From ref. [44].

double bonds. To develop a more accurate predictive correlation of binary diffusion coefficients, the effects of solute polarity should be taken into account and more data needs to be accumulated.

4. Conclusions

The impulse response techniques, which include the Taylor dispersion, modified Taylor dispersion, and chromatographic impulse response (CIR) method, are effective for the determination of binary diffusion coefficients under supercritical conditions. In the CIR method, solute retention factor and PMV, which in the latter is derived from the retention factor, also can be determined. For each impulse response method, the theoretical background, accuracy of the parameter determined, and error sources were discussed. The curve-fitting method was found superior to the moment method for the analysis of the response curve. To improve the determined values, a correction for secondary flow effects due to column coiling, and noise elimination in response signals with low absorbance intensities were described. Based on our recent measurements of binary diffusion coefficients, predictive correlations based on the Schmidt number and diffusion coefficient-viscosity correlations are recommended.

5. Nomenclature

a, a^*	defined by Eqs. (25) and (33), respectively ($m^2\,s^{-1}$)
$c(r, x, t)$	tracer concentration in cylindrical tube ($mol\,m^{-3}$)
$C(x,t)$	cross-sectional average concentration, defined by Eq. (5) ($mol\,m^{-3}$)
$C_{app}(x, t)$	approximate average concentration given by Eq. (10) or Eq. (24) ($mol\,m^{-3}$)
D_{1m}	pseudo binary diffusion coefficient in mixed solvent ($m^2\,s^{-1}$)
D_{12}	binary diffusion coefficient ($m^2\,s^{-1}$)
D'_{12}	apparent binary diffusion coefficient including secondary flow effect ($m^2\,s^{-1}$)
$D_{12,0}$	binary diffusion coefficient based on the Taylor dispersion ($m^2\,s^{-1}$)
D_s	surface diffusion coefficient ($m^2\,s^{-1}$)
De	Dean number ($= (2R\rho u_a/\eta)\lambda^{1/2}$)
$f(t)$	given by Eq. (17) (s^{-1})
$F(s)$	transfer function defined by Eq. (18)
k	retention factor for polymer layer to supercritical fluid
k'	apparent retention factor including secondary flow effect
K	defined by Eq. (7) ($m^2\,s^{-1}$)
L	column length (m)
m	total amount of tracer input (mol)
M	molecular weight
P	pressure (Pa)
r	radial distance variable (m)
R	tube radius (m)
R_g	gas constant ($J\,K^{-1}\,mol^{-1}$)
s	Laplace operator (s^{-1})
Sc	Schmidt number ($= \eta/(\rho D_{12})$)
Sc^+	ratio of Schmidt number at high pressure to that at atmospheric pressure
t	time (s)
t_1, t_2	time at 10% peak height of response curve ($t_1 < t_2$) (s)
T	temperature (K)
u_a	average fluid velocity ($m\,s^{-1}$)
v	solvent molar volume ($m^3\,mol^{-1}$)
v_0	hard-sphere closest-packed volume ($m^3\,mol^{-1}$)
v_m^∞	infinite dilution solute partial molar volume in fluid phase ($m^3\,mol^{-1}$)
v_s^∞	infinite dilution solute partial molar volume in polymer phase ($m^3\,mol^{-1}$)
x	axial distance variable (m)
x_2, x_3	mole fraction

Greek symbols

α, β	constant defined by Eq. (39)
β_T	isothermal compressibility (Pa^{-1})
$\delta(t)$, $\delta(x)$	Dirac's delta function (s^{-1} and m^{-1}, respectively)
ε	root-mean-square error defined by Eq. (11)
η	viscosity (Pa s)
λ	ratio of tube radius to coil radius
ρ	density ($kg\,m^{-3}$)
σ	hard-sphere diameter (m)
σ^2	second order temporal moment (s^2)

Superscripts

I	input
II	output

Subscripts

exp	experiment
vw	van der Waals
1	solute
2, 3	solvent

Acknowledgements

This work was financially supported by the Ministry of Education, Culture, Sports, Science and Technology of Japan through Grant-in-Aids for Scientific Research (No. 14655284 and No.15560658).

References

[1] M.B. Iomtev, Y.V. Tsekhanskaya, Russ. J. Phys. Chem. 38 (1964) 485.
[2] Y.V. Tsekhanskaya, Russ. J. Phys. Chem. 45 (1971) 744.
[3] I. Swaid, G.M. Schneider, Ber. Bunsenges. Phys. Chem. 83 (1979) 969.
[4] K.K. Liong, P.A. Wells, N.R. Foster, J. Supercrit. Fluids 4 (1991) 91.
[5] J.J. Suárez, I. Medina, J.L. Bueno, Fluid Phase Equilib. 153 (1998) 167.
[6] T. Funazukuri, H. Nishiumi, in: Y. Arai, T. Sako, Y. Takebayashi (Eds.), Supercritical Fluids, Springer, Berlin, 2002, pp. 172–193.
[7] G. Taylor, Proc. R. Soc. Lond. A219 (1953) 186.
[8] R. Aris, Proc. R. Soc. Lond. A235 (1956) 67.
[9] H.J.V. Tyrrell, K.R. Harris, Diffusion in Liquids, Butterworths, London, 1984, pp. 193–199.
[10] A.N. Berezhnoi, A.V. Semenov, Binary Diffusion Coefficients of Liquid Vapors in Gases, Begell House, New York, 1997, pp. 14–17.
[11] C. Erkey, A. Akgerman, in: W.A. Wakeham, A. Nagashima, J.V. Sengers (Eds.), Measurement of the Transport Properties of Fluids, Blackwell, Oxford, 1991, pp. 251–265.
[12] W.A. Wakeham, A. Nagashima, J.V. Sengers (Eds.), Measurement of the Transport Properties of Fluids, Blackwell, Oxford, 1991, p. 233.
[13] T. Funazukuri, C.Y. Kong, S. Kagei, Fluid Phase Equilib. 194–197 (2002) 1169.
[14] T. Funazukuri, C.Y. Kong, N. Murooka, S. Kagei, Ind. Eng. Chem. Res. 39 (2000) 4462.
[15] C.Y. Kong, T. Funazukuri, S. Kagei, J. Chromatogr. A 1035 (2004) 177.
[16] S. Umezawa, A. Nagashima, J. Supercrit. Fluids 5 (1992) 242.
[17] H. Nishiumi, M. Fujita, K. Agou, Fluid Phase Equilib. 117 (1996) 356.
[18] K. Ago, H. Nishiumi, J. Chem. Eng. Jpn. 32 (1999) 563.
[19] X.N. Yang, L.A.F. Coelho, M.A. Matthews, Ind. Eng. Chem. Res. 39 (2000) 3059.
[20] T. Funazukuri, C.Y. Kong, S. Kagei, Int. J. Thermophys. 22 (2001) 1643.
[21] J.M.H. Levelt Sengers, U.K. Deiters, U. Klask, P. Swidersky, G.M. Schneider, Int. J. Thermophys. 14 (1993) 893.
[22] T. Funazukuri, C.Y. Kong, S. Kagei, Ind. Eng. Chem. Res. 39 (2000) 835.
[23] A.A. Clifford, S.E. Coleby, Proc. R. Soc. Lond. A433 (1991) 63.
[24] T. Funazukuri, C.Y. Kong, S. Kagei, Int. J. Thermophys. 21 (2000) 651.
[25] T. Funazukuri, C.Y. Kong, S. Kagei, Int. J. Thermophys. 21 (2000) 1279.
[26] N. Wakao, S. Kaguei, Heat and Mass Transfer in Packed Beds, Gordon Breach, New York, 1982, p. 17.
[27] N. Dahmen, A. Kordikowski, G.M. Schneider, J. Chromatogr. 505 (1990) 169.
[28] O.J. Catchpole, M.B. King, Ind. Eng. Chem. Res. 33 (1994) 1828.
[29] K. Arai, S. Saito, S. Maeda, Kagaku Kogaku (Jpn. J. Chem. Eng.) 32 (1968) 354.
[30] P.R. Sassiat, P. Mourier, M.H. Caude, R.H. Rosset, Anal. Chem. 59 (1987) 1164.
[31] J.L. Bueno, J.J. Suárez, J. Dizy, I. Medina, J. Chem. Eng. Data 38 (1993) 344.
[32] T. Funazukuri, N. Nishimoto, Fluid Phase Equilib 125 (1996) 235.
[33] H.H. Lauer, D. McManigill, R.D. Board, Anal. Chem. 55 (1983) 1370.
[34] S.V. Olesik, J.L. Steger, N. Kiba, M. Roth, M.V. Novotny, J. Chromatogr. 392 (1987) 165.
[35] M. Roth, J. Phys. Chem. 96 (1992) 8522.
[36] M. Roth, Fluid Phase Equilib. 148 (1998) 189.
[37] M.J.E. Golay, in: Proceedings of the Second Symposium on Gas Chromatography, Academic Press, New York, 1958, pp. 36–55.
[38] M.J.E. Golay, Anal. Chem. 29 (1957) 928.
[39] C.C. Lai, C.S. Tan, Ind. Eng. Chem. Res. 34 (1995) 674.
[40] T. Funazukuri, C.Y. Kong, S. Kagei, J. Supercrit. Fluids 27 (2003) 85.
[41] T. Funazukuri, C.Y. Kong, S. Kagei, Ind. Eng. Chem. Res. 41 (2002) 2812.
[42] T. Funazukuri, C.Y. Kong, S. Kagei, Fluid Phase Equilib. 206 (2003) 163.
[43] T. Funazukuri, C.Y. Kong, T. Kikuchi, S. Kagei, J. Chem. Eng. Data 48 (2003) 684.
[44] T. Funazukuri, C.Y. Kong, S. Kagei, Fluid Phase Equilib. 219 (2004) 67.
[45] T. Funazukuri, C.Y. Kong, S. Kagei, Fluid Phase Equilib. (2004) in press.
[46] T. Funazukuri, C.Y. Kong, S. Kagei, Chem. Eng. Sci. (2004) in press.
[47] C. Erkey, H. Gadalla, A. Akgerman, J. Supercrit. Fluids 3 (1990) 180.
[48] W.R. Dean, Phil. Mag. 5 (1928) 673.
[49] A. Alizadeh, C.A. Nieto de Castro, W.A. Wakeham, Int. J. Thermophys. 1 (1980) 243.
[50] P.G. Debenedetti, R.C. Reid, in: J.M.L. Penninger, R. Radosz, M.A. McHugh, V.J. Krukonis, Eds., Supercritical Fluid Technology, Elsevier, Amsterdam, 1985, pp. 225–244.
[51] T. Funazukuri, S. Hachisu, N. Wakao, Ind. Eng. Chem. Res. 30 (1991) 1323.
[52] T. Funazukuri, Y. Ishiwata, N. Wakao, AIChE J. 38 (1992) 1761.
[53] U. Wasen, I. Swaid, G.M. Schneider, Angew. Chem., Int. Ed. Engl. 19 (1980) 575.
[54] A. Crevatin, A. Zwahlem, I. Kikic, J. Supercrit. Fluids 12 (1998) 99.
[55] S.A. Smith, V. Shenai, M.A. Matthews, J. Supercrit. Fluids 3 (1990) 175.
[56] S.V. Olesik, J.L. Woodruff, Anal. Chem. 63 (1991) 670.
[57] T. Funazukuri, Y. Ishiwata, N. Wakao, J. Chem. Eng. Jpn. 24 (1991) 387.
[58] V.M. Shenai, B.L. Hamilton, M.A. Matthews, in: E. Kiran, J.F. Brennecke (Eds.), Supercritical Fluid Engineering Science-Fundamental and Applications (ACS Symposium Series No. 514), American Chemical Society, Washington, DC, 1993, pp. 92–103.
[59] T. Funazukuri, Y. Ishiwata, Fluid Phase Equilib. 164 (1999) 117.
[60] L.M. González, J.L. Bueno, I. Medina, J. Supercrit. Fluids 24 (2002) 219.
[61] S.T. Lee, S.V. Olesik, Anal. Chem. 66 (1994) 4498.
[62] I. Souvignet, S.V. Olesik, Anal. Chem. 70 (1998) 2783.
[63] C. Mantell, M. Rodríguez, E. Martínez de la Ossa, J. Supercrit. Fluids 25 (2003) 57.

[64] T. Funazukuri, N. Nishimoto, N. Wakao, J. Chem. Eng. Data 39 (1994) 911.
[65] R.C. Reid, J.M. Prausnitz, B.E. Poling, The Properties of Gases and Liquids, McGraw-Hill, New York, 4th ed., 1987, p. 432.
[66] R. Feist, G.M. Schneider, Sep. Sci. Technol. 17 (1982) 261.
[67] T.J. Bruno, J. Res. Natl. Inst. Stand. Technol. 94 (1989) 105.
[68] T. Funazukuri, S. Hachisu, N. Wakao, Anal. Chem. 61 (1989) 118.
[69] N. Dahmen, A. Dülberg, G.M. Schneider, Ber. Bunsenges. Phys. Chem. 94 (1990) 384.
[70] T.J. Bruno, in: T.J. Bruno, J.F. Ely (Eds.), Supercritical Fluid Technology, CRC Press, New York, 1991, p. 293–323.
[71] K.K. Liong, P.A. Wells, N.R. Foster, Ind. Eng. Chem. Res. 30 (1991) 1329.
[72] K.K. Liong, P.A. Wells, N.R. Foster, Ind. Eng. Chem. Res. 31 (1992) 390.
[73] T. Wells, N.R. Foster, R.P. Chaplin, Ind. Eng. Chem. Res. 31 (1992) 927.
[74] J.J. Suárez, J.L. Bueno, I. Medina, Chem. Eng. Sci. 48 (1993) 2419.
[75] A. Akgerman, C. Erkey, M. Orejuela, Ind. Eng. Chem. Res. 35 (1996) 911.
[76] T. Funazukuri, J. Chem. Eng. Jpn. 29 (1996) 191.
[77] C.M. Silva, E.A. Macedo, Ind. Eng. Chem. Res. 37 (1998) 1490.
[78] K.A. Rezaei, F. Temelli, J. Supercrit. Fluids 17 (2000) 35.
[79] H. Fu, L.A.F. Coelho, M.A. Matthews, J. Supercrit. Fluids 18 (2000) 141.
[80] X.N. Yang, M.A. Matthews, J. Chem. Eng. Data 46 (2001) 588.
[81] L.M. González, J.L. Bueno, I. Medina, Ind. Eng. Chem. Res. 40 (2001) 3711.
[82] C.A. Filho, C.M. Silva, M.B. Quadri, E.A. Macedo, J. Chem. Eng. Data 47 (2002) 1351.
[83] C.A. Filho, C.M. Silva, M.B. Quadri, E.A. Macedo, Fluid Phase Equilib. 204 (2003) 65.
[84] L.A.F. Coelho, J.V. de Oliveira, F.W. Tavares, M.A. Matthews, Fluid Phase Equilib. 194–197 (2002) 1131.
[85] M.A. Matthews, J.M. Becnel, J. Chem. Eng. Data 48 (2003) 1413.
[86] S.R. Springston, M. Novotny, Anal. Chem. 56 (1984) 1762.
[87] A. Kopner, A. Hamm, J. Ellert, R. Feist, G.M. Schneider, Chem. Eng. Sci. 42 (1987) 2213.
[88] J.M. Noel, C. Erkey, D.B. Bukur, A. Akgerman, J. Chem. Eng. Data 39 (1994) 920.
[89] A. Eaton, D.B. Bukur, A. Akgerman, J. Chem. Eng. Data 40 (1995) 1293.
[90] A.P. Eaton, A. Akgerman, Ind. Eng. Chem. Res. 36 (1997) 923.
[91] V.S. Morozov, E.G. Vinkler, Russ. J. Phys. Chem. 49 (1975) 1404.
[92] E.G. Vinkler, V.S. Morozov, Russ. J. Phys. Chem. 49 (1975) 1405.
[93] D.Q. Tuan, M.E. Yener, J.A. Zollweg, P. Harriott, S.S.H. Rizvi, Ind. Eng. Chem. Res. 38 (1999) 554.
[94] G. Knaff, E.U. Schlünder, Chem. Eng. Process. 21 (1987) 101.
[95] H. Higashi, Y. Iwai, Y. Takahashi, H. Uchida, Y. Arai, Fluid Phase Equilib. 144 (1998) 269.
[96] H. Higashi, Y. Iwai, Y. Nakamura, S. Yamamoto, Y. Arai, Fluid Phase Equilib. 166 (1999) 101.
[97] S. Tahakashi, H. Iwasaki, Rev. Phys. Chem. Jpn. 38 (1968) 28.
[98] S. Takahashi, Bull. Chem. Soc. Jpn. 47 (1968) 1573.
[99] S. Takahashi, Bull. Chem. Soc. Jpn. 45 (1972) 2074.
[100] S. Takahashi, Bull. Chem. Soc. Jpn. 47 (1974) 1342.
[101] S. Takahashi, H. Hongo, J. Chem. Eng. Jpn. 15 (1982) 57.
[102] H. Saad, E. Gulari, Ber. Bunsenges. Phys. Chem. 88 (1984) 834.
[103] D.M. Lamb, S.T. Adamy, K.W. Woo, J. Jonas, J. Phys. Chem. 93 (1989) 5002.
[104] T. Funazukuri, N. Wakao, Preprint for the AIChE Annual Meeting at St. Louis, 1993.
[105] A. Bondi, J. Phys. Chem. 68 (1964) 441.